applied sciences

MDPI

Article

Active Control of Low-Frequency Noise through a Single Top-Hung Window in a Full-Sized Room

Bhan Lam [1,*], Dongyuan Shi [1], Valiantsin Belyi [1], Shulin Wen [1], Woon-Seng Gan [1], Kelvin Li [2] and Irene Lee [2]

1 School of Electrical and Electronic Engineering, Nanyang Technological University, Singapore 639798, Singapore; dshi003@e.ntu.edu.sg (D.S.); bely0001@e.ntu.edu.sg (V.B.); alicia.wen@ntu.edu.sg (S.W.); ewsgan@ntu.edu.sg (W.-S.G.)

2 Building & Research Institute, Housing & Development Board, Singapore 738973, Singapore; kelvin_wh_li@hdb.gov.sg (K.L.); irene_yl_lee@hdb.gov.sg (I.L.)

* Correspondence: blam002@e.ntu.edu.sg

Received: 14 September 2020; Accepted: 25 September 2020; Published: 29 September 2020

Featured Application: An active control approach to mitigate low-frequency noise propagating through an open top-hung window, while allowing natural ventilation.

Abstract: The push for greater urban sustainability has increased the urgency of the search for noise mitigation solutions that allow for natural ventilation into buildings. Although a viable active noise control (ANC) solution with up to 10 dB of global attenuation between 100 Hz and 1000 Hz was previously developed for an open window, it had limited low-frequency performance below 300 Hz, owing to the small loudspeakers used. To improve the low-frequency attenuation, four passive radiator-based speakers were affixed around the opening of a top-hung ventilation window. The active control performance between 100 Hz and 700 Hz on a single top-hung window in a full-sized mock-up apartment room was examined. Active attenuation came close to the performance of the passive insulation provided by fully closing the window for expressway traffic and motorbike passing noise types. For a jet aircraft flyby, the performance of active attenuation with the window fully opened was similar to that of passive insulation with fully closed windows. In the case of low-frequency compressor noise, active attenuation's performance was significantly better than the passive insulation. Overall, between 8 dB and 12 dB of active attenuation was achieved directly in front of the window opening, and up to 10.5 dB of attenuation was achieved across the entire room.

Keywords: active noise control; natural ventilation; façade insulation; noise pollution

1. Introduction

The World Health Organization (WHO) has recently put forth strong recommendations to reduce urban transportation noise levels. These recommendations are underpinned by a rapidly growing body of evidence associating a myriad of health risks with environmental noise exposure [1]. In high-rise urban landscapes, traditional noise mitigation approaches, such as noise barriers, have limited efficacy in the low-frequency range and are effective only for the lower floors of a high-rise building that are in its shadow zone [2]. Although noise mitigation at the receivers' end, such as on building façades, is inefficient, it is usually the only form noise control available for land-scarce, high-density urban cities. The sustainability push for naturally ventilated buildings also increases noise control difficulty, as noise propagates easily through any opening in the façade.

Noise control for naturally ventilated buildings has been traditionally passive, wherein physical elements have been employed to obstruct or dampen the acoustic waves as they enter the façade [3,4].

The main limitation of effective passive interventions, such as louvres and plenum windows, appears to be the restriction of airflow. Moreover, passive elements are designed with the noise control perspective of reducing the total acoustic pressure in the building interior by treating all sounds that enter the façade opening as waste to be reduced. Although the indoor acoustic environment for naturally ventilated buildings is dependent on context, there has been some evidence showing a preference of some external sound sources (e.g., natural sounds, human voices) over others (e.g., heavy traffic) while no indoor sound sources were present [5]. With the introduction of international standards on soundscapes [6–8], it is imperative that indoor acoustic comfort is approached with a perceptual perspective [9]. One overlooked factor in an indoor environment is the concept of control, which is challenging for naturally ventilated buildings. For instance, opening windows to lower the temperature increases the influx of exterior noise. The selective control of external noise sources [10–12] without obstructing airflow appears to be achievable with an active noise control (ANC) system designed for façade openings [13].

By projecting an opposing sound wave with the same amplitude at the precise time and space of the disturbance to be controlled, ANC has been successfully integrated into automobile cabins [14,15], aircraft cabins [16], and headsets [17] to reduce low-frequency noise. The ANC principle has been recently adapted for façade openings to provide significant noise control without obstruction to natural ventilation [13,18–20]. Even though the proposed method where noise sources are distributed across the entire aperture allows for optimal control [21], the limited size of the loudspeakers in such a layout inherently limits noise control performance in the low frequency range.

To improve low-frequency active control performance, larger loudspeakers were affixed to a full-sized, but smaller, top-hung ventilation window. Active control of recorded urban noise was evaluated in a full-scale room of a mockup residential apartment. For comparison, the active control performance was benchmarked to the passive insulation provided by fully closing the window.

2. Materials and Methods

2.1. Experimental Setup

The active control system was installed on a single 60 cm × 40 cm top-hung window above a full-sized apartment window, as shown in Figure 1a. A single reference microphone (PylePro PLM3, Pyle Audio Inc., New York, NY, USA) sensed the primary noise from a single loudspeaker (8341A, Genelec Oy, Iisalmi, Finland), located in an adjoining 270 cm × 340 cm × 260 cm chamber outside the window, as depicted in Figure 1b. The reference signal was fed into the controller (NI 8135, National Instruments, Austin, TX, USA), which drove four control loudspeakers (T3-2190S, TB Speaker Co. Ltd., Taipei, Taiwan) to actively minimize the sum-of-the-squared pressures at four error microphones (PylePro PLM3).

An array of six microphones (GRAS 40PH, GRAS Sound & Vibration A/S, Holte, Denmark) was distributed across the entire 287.5 cm × 525 cm × 260 cm room to evaluate the global control performance in the entire room, as denoted by the microphones numbered from 1 to 6 in Figure 2. These six microphones were arranged based on the recommendations in ISO 16283-3:2016 [22]. The seventh observation microphone (GRAS 40PH) was mounted in the center of the error microphone array, which was 30 cm from the window aperture, to evaluate the performance at the error microphone positions.

As the chamber where the primary source was located was designed as a reverberation chamber, both doors were left open to release some of the acoustic modes. The doors in the receiving room were kept closed during the experiment.

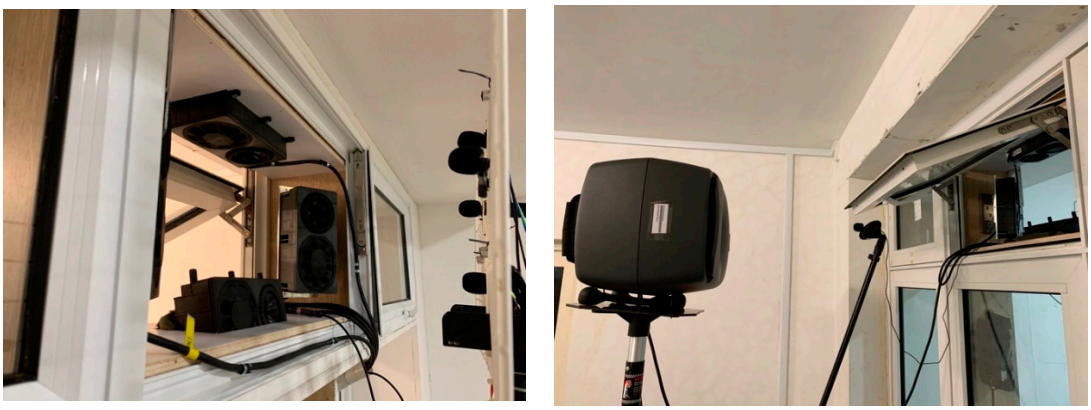

(**a**) (**b**)

Figure 1. (**a**) Layout of the four secondary sources around a customized wooden frame and four error microphones placed 30 cm away, and (**b**) the primary source and reference microphone on the outside of the fully opened top-hung window.

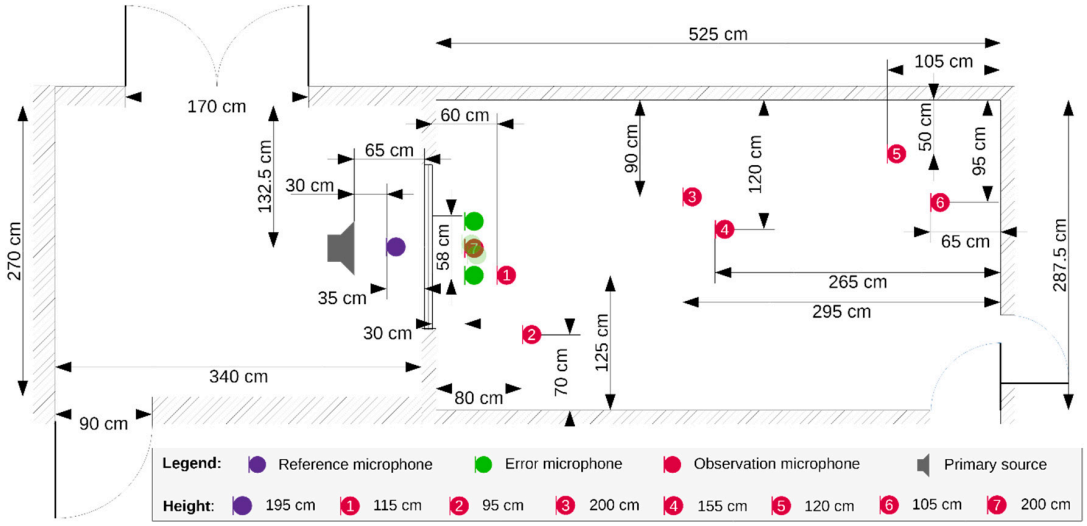

Figure 2. Room dimensions, observation microphone layout, primary source, reference microphone, and error microphone placement.

2.2. Active Control Formulation

A multichannel, feedforward filtered-x least mean square (FXLMS) algorithm was adopted, as illustrated by the block diagram in Figure 3 [23]. A single reference microphone ($J = 1$) provided advanced information of the impinging noise to $K = 4$ control filters, which drove $K = 4$ control sources to minimize the sum-of-the-squared pressures at the $M = 4$ error microphones. The mth error microphone signal $e_m(n)$ can be expressed as

$$e_m(n) = d_m(n) - \sum_{k=1}^{K} s_{mk}(n) * \left[\boldsymbol{w}_k^{\mathrm{T}}(n)\boldsymbol{x}(n)\right], \tag{1}$$

where $d_m(n) = p_m(n) * x(n)$ is the disturbance to be cancelled at the mth error microphone and $s_{mk}(n)$ is the real secondary path transfer function from the kth control source to the mth error microphone. $\boldsymbol{w}_k(n) = \begin{bmatrix} w_{k,0}(n) & w_{k,1}(n) & \cdots & w_{k,L-1}(n) \end{bmatrix}^{\mathrm{T}}$ is the coefficient vector of the control filter with order

L, and $\boldsymbol{x}(n) = \begin{bmatrix} x(n) & x(n-1) & \cdots & x(n-L+1) \end{bmatrix}^{\mathrm{T}}$ is the reference signal vector of **W**(z). The kth equation of the FXLMS algorithm is given by

$$w_k(n+1) = \boldsymbol{w}_k(n) + \mu \sum_{m=1}^{M} \boldsymbol{x}'_{km}(n) e_m(n), \tag{2}$$

where μ is the step size and $\boldsymbol{x}'_{km}(n) = \hat{s}_{mk}(n) * \boldsymbol{x}(n)$ is the filtered reference signal from the measured secondary path estimate $\hat{s}_{mk}(n)$. Hence, the kth secondary source output is given by

$$\boldsymbol{y}_k(n) = \boldsymbol{w}_k^{\mathrm{T}}(n) * \boldsymbol{x}(n). \tag{3}$$

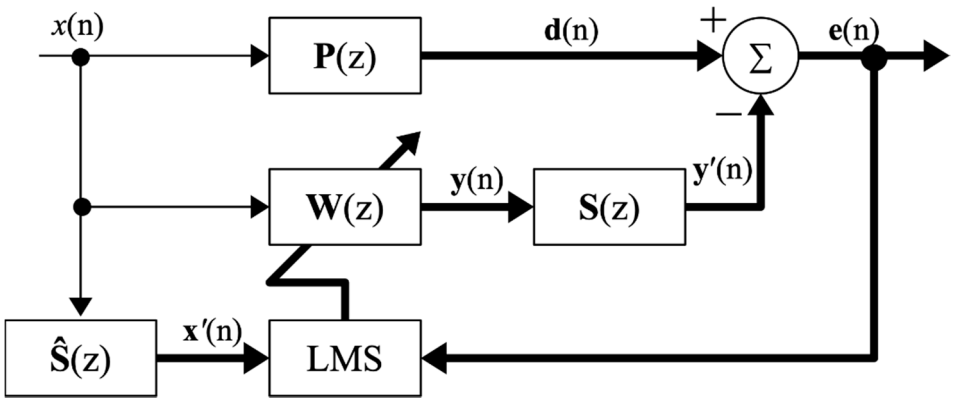

Figure 3. Block diagram of the active noise control system.

The parameters used in the execution of the FXLMS algorithm are summarized in Table 1. The filter order and sampling rate were maximized to fully utilize the available resources on the real-time platform described in Section 2.1. The control filter length was also maximized to account for the non-ideal acoustic conditions described in the following section.

Table 1. Active control parameters.

Reference microphones	$J = 1$
Control sources and filters	$K = 4$
Error microphones	$M = 4$
Sampling rate	16,000 Hz
Control filter length, $L + 1$	640
Secondary path length	256
Step size	1×10^{-11}

2.3. System Characteristics

The impulse response of the primary paths was measured from the reference microphone at the periphery of the opened top-hung window panel (see Figure 1b) to each of the four error microphones, with the measurements shown in Figure 4a. The reverberations in the adjacent chamber, where the primary noise was placed, were reflected in the jitter of the impulse responses. There was also a prominent mode at around 300 Hz, as portrayed in the frequency response of the primary paths, shown in Figure 4b. This was despite keeping the doors open to release the modes and employing unidirectional microphones for both the reference and error microphones.

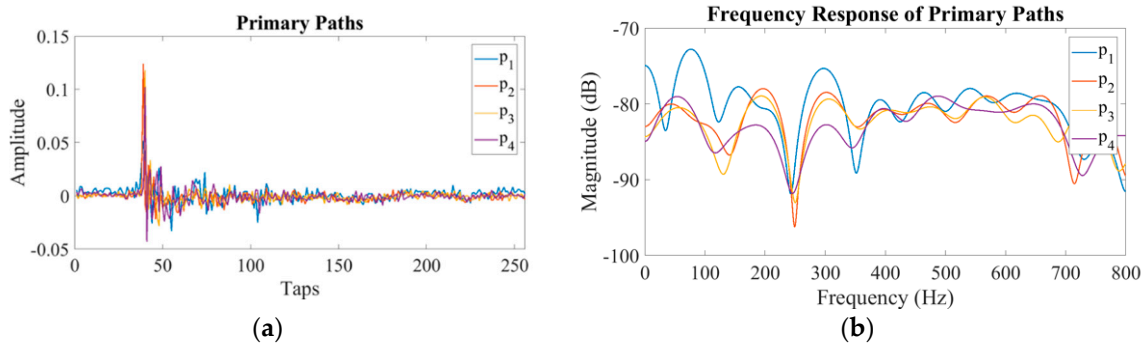

Figure 4. (**a**) Impulse response of the primary paths measured from the reference microphone to each of the four error microphones, and (**b**) the corresponding frequency responses.

The same jitter was also observed in the secondary paths. These secondary paths were measured from each of the speakers to each error microphone to obtain a total of 16 transfer functions (i.e., s_{mk}), as shown in Figure 5. It seemed that only the secondary paths at the third error microphone were adversely affected by the acoustic mode at 300 Hz, as shown in Figure 6c. Despite the jitter and acoustic mode observed, preliminary tests indicated that the acoustic conditions were satisfactory for the control filters to converge.

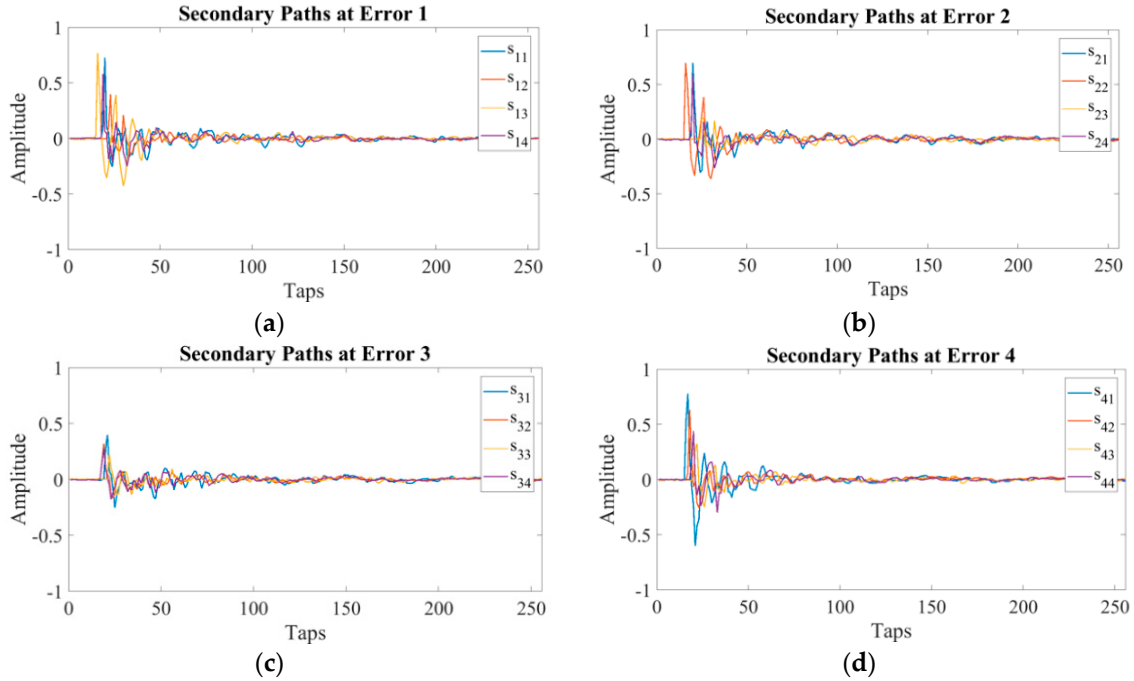

Figure 5. Offline measurements of the secondary paths from the four loudspeakers to error microphones (**a**) 1, (**b**) 2, (**c**) 3, and (**d**) 4.

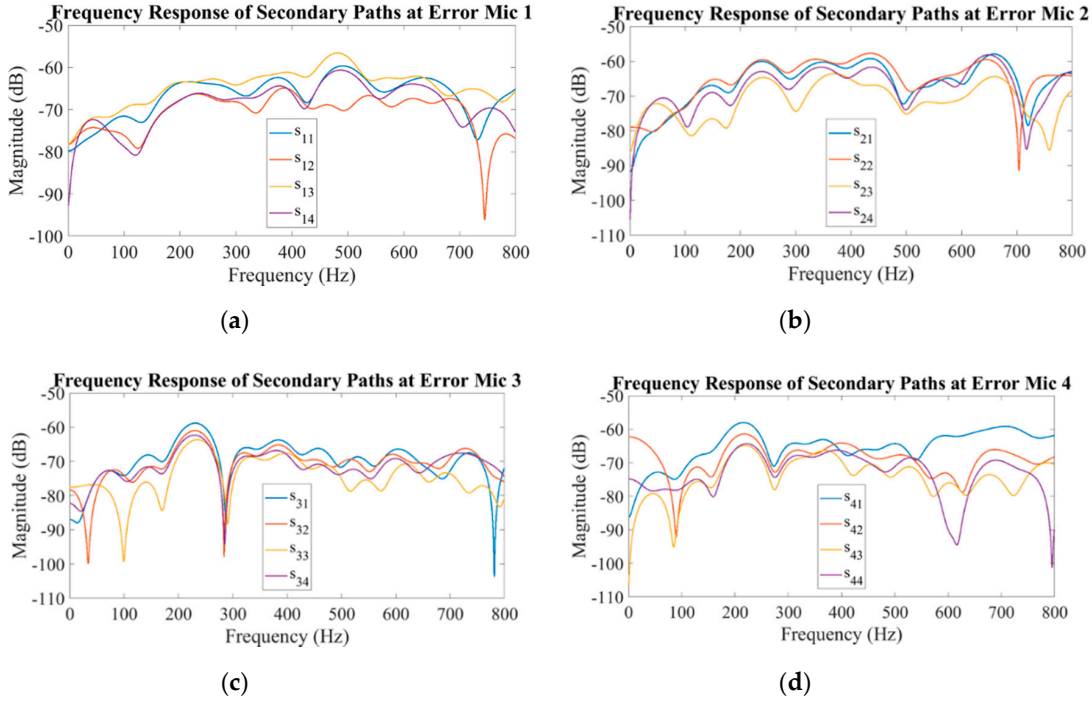

Figure 6. Frequency responses of the secondary paths from the four loudspeakers to error microphones (**a**) 1, (**b**) 2, (**c**) 3, and (**d**) 4.

2.4. Primary Noise Types

A total of four representative primary noise samples were employed in the evaluation of the active control system. These noise samples were a representation of common urban noises in Singapore with dominant low-frequency content. All but the compressor noise was recorded on a window panel with a surface microphone (GRAS 147AX, GRAS Sound & Vibration A/S, Holte, Denmark). The compressor noise was recorded next to an industrial air conditioning compressor on the roof of the university building with a handheld recorder (Zoom H6, Zoom Corporation, Chiyoda, Tokyo, Japan). Both the aircraft flyby and the traffic noises were recorded in residential districts, whereas the motorbike passing noise was recorded in an industrial district. The duration of each of passing noise sample reflected the entire buildup, whereas the duration was selected to be longer than 6 s for stationary noises, according to ISO 16283-3. The dominant frequencies of the aircraft flyby noise seemed to occur between 200 Hz and 400 Hz in one-third octave bands, as shown in Figure 7a. There were prominent tonal components in the motorbike and compressor noises, as illustrated in Figure 7b,d, respectively. The energy appeared to be evenly distributed between 160 Hz and 630 Hz in one-third octave bands in traffic noise, as shown in Figure 7c.

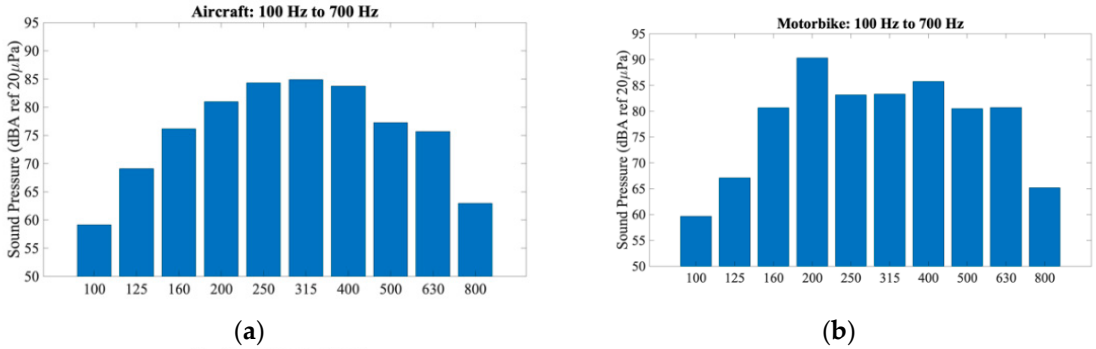

Figure 7. *Cont.*

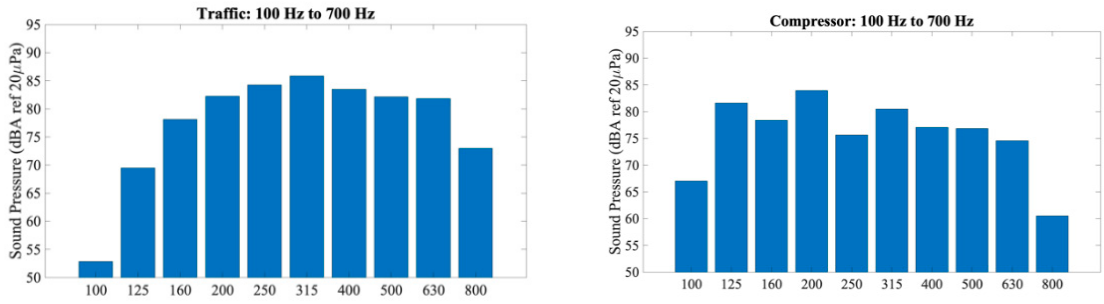

Figure 7. One-third octave band spectra at observation microphone 7 for (**a**) aircraft, (**b**) motorbike, (**c**) traffic, and (**d**) compressor noise.

2.5. Evaluation Criteria

The space and time average sound pressure level (SPL) in the room is defined as the energy-average sound pressure level, L_{EA}, in the receiving room, given by

$$L_{EA} = 10 \log_{10}\left(\frac{1}{n}\sum_{i=1}^{n} 10^{L_{Aeq,i}/10}\right), \tag{4}$$

where $L_{Aeq,i}$ is the A–weighted equivalent SPL at the ith microphone position (i.e., $n = 6$) in the room [22]. The energy–average attenuation due to the ANC system with the windows fully opened is written as

$$\alpha_{active,EA} = L_{EA,Off} - L_{EA,On}, \tag{5}$$

where $L_{EA,Off}$ and $L_{EA,On}$ are the energy–average SPLs with the ANC system turned off and on, respectively, both while the windows were fully opened. It follows that the passive attenuation is given by

$$\alpha_{passive,EA} = L_{EA,Off} - L_{EA,Closed}, \tag{6}$$

where $L_{EA,Closed}$ is the energy-average SPL with the ANC system turned off and with the windows fully closed.

Similarly, the active and attenuation at the seventh observation microphone near the error microphones can be written as

$$\alpha_{active,Error} = L_{Aeq,7,Off} - L_{Aeq,7,On}. \tag{7}$$

The passive attenuation at the seventh observation microphone near the error microphones can be expressed as

$$\alpha_{passive,Error} = L_{Aeq,7,Off} - L_{Aeq,7,Closed}. \tag{8}$$

It is important to note that, since all four primary noise types were temporally different, the duration for the equivalent sound pressure level (L_{Aeq}) calculation was track-dependent (i.e., 47.2 s for aircraft noise and 10 s for compressor noise). This ensured that the attenuation was measured across the entire sound event, especially for transient noise sources such as aircraft flyby and motorbike passing noises.

3. Results

For repeatability in the measurement of the attenuation, and to mimic practical realization of such an active control system on domestic windows, a fixed-filter approach was adopted. Each primary noise type was played on loop to allow the FXLMS algorithm to converge to a steady state, after which the control filter coefficients were stored. The control signals were generated by convolving the reference signal with the stored fixed-coefficient finite impulse response (FIR) filters, i.e., $\boldsymbol{y}_k(n) = \boldsymbol{w}^{\mathrm{T}}_{k,fixed}(n) * \boldsymbol{x}(n)$,

where $\boldsymbol{w}_{k,fixed}(n)$ is the kth fixed-coefficient control filter. Hence, the active control attenuation performance of the fixed-filter implementation measured the instantaneous steady state attenuation across the entire duration of the primary noise.

3.1. Passive and Active Attenuation Performance

As the ANC system is designed to minimize the sum-of-the-squared sound pressure levels at the error microphone positions, the active control performance of the four primary noise types (see Table 2) is first evaluated at the seventh observation microphone, placed near the error microphones. The active and passive attenuation at the seventh observation microphone, $\alpha_{active,Error}$ and $\alpha_{passive,Error}$, respectively, are summarized in Table 3. Across the four primary noise types, active attenuation was somewhat consistent (8 dB to 12 dB), whereas the passive attenuation was about 10 dB, with the exception of compressor noise. The passive attenuation of the compressor noise was only 6.5 dB, which was about half that of the active attenuation at 12.4 dB.

Table 2. Characteristics of the primary noise samples.

Noise Types	Aircraft	Motorbike	Traffic	Compressor
Duration, s	47.2	16.41	13.19	10
Frequency range, Hz	100 to 700	100 to 700	100 to 700	100 to 700
Recording location	Residential	Industrial	Residential	University
Description	Jet aircraft flyby	Motorbike passing by	Non-peak traffic from expressway	Adjacent to source

Table 3. Sound pressure level attenuation in dB of observation microphone 7 near the error microphones, and the energy-average across six microphones (microphones 1–6) across the four noise types, with ANC turned on (window opened) and ANC turned off (window closed).

Mode of Operation		Attenuation of Primary Noise Types (dB)			
		Aircraft	Motorbike	Traffic	Compressor
ANC ON (window opened)	$\alpha_{active,Error}$	9.5	8.97	7.99	12.36
	$\alpha_{active,EA}$	5.76	4.84	4.56	10.51
ANC OFF (window closed)	$\alpha_{passive,Error}$	9.98	10.09	10.77	6.47
	$\alpha_{passive,EA}$	5.66	6.57	6.45	4.85

To evaluate the global control effectiveness of the ANC system, the active and passive attenuation, calculated with the energy-average SPL of microphones one through six (see Figure 2) are also presented in Table 3. The active and passive attenuation (i.e., $\alpha_{active,EA}$ and $\alpha_{passive,EA}$) were almost 4 dB lower than at the error microphone position, except for the compressor noise. However, the trend across the noise types was similar to that of the attenuation at the error microphone position. Overall, the ANC system on a fully opened top-hung window offered similar attenuation to the passive insulation provided by fully closing the window. More importantly, active attenuation outperformed passive attenuation significantly for compressor noise.

3.2. Attenuation Performance as a Function of Frequency

To understand the frequency dependency of the attenuation performance for both the ANC system and the passive insulation of the fully shut window, the attenuation level at the seventh microphone was plotted as a function of frequency, as shown in Figure 8. In the low frequencies, the active control performance exceeded that of the passive insulation up to about 250 Hz across all noise types. Attenuation of the aircraft noise between active and passive control was similar across the entire frequency band, with ANC providing better reduction in the lower frequencies, as shown in Figure 8a.

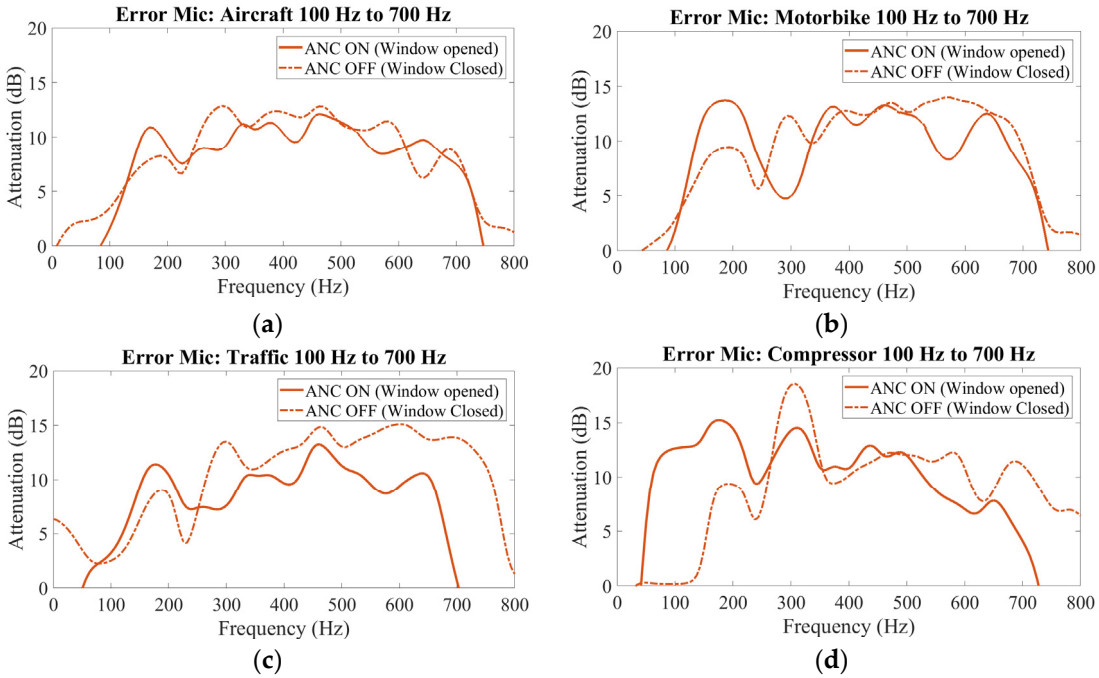

Figure 8. Attenuation in dB at microphone 7 as a function of frequency with ANC ON (window opened) and ANC OFF (window closed) across (**a**) aircraft, (**b**) motorbike, (**c**) traffic, and (**d**) compressor noise types.

There was a significant roll-off in ANC attenuation at 300 Hz for the motorbike noise, as shown in Figure 8b. This dip in ANC performance at 300 Hz was observed for all four noise types, which could be due to the 300 Hz mode observed in the primary and secondary paths. In the case of the compressor noise, active control significantly outperformed passive insulation up to about 250 Hz, with a match in performance between 350 Hz and 500 Hz, which explains the results in Table 3. Moreover, passive control was negligible up to about 150 Hz, as shown in Figure 8d. In general, passive control outperformed the active control system above roughly 500 Hz, which was reflected in all the primary noise types.

Energy-average attenuation performances (i.e., microphones 1–6) were in line with that found near the error microphone position (microphone 7), where the active control nearly matched that of the passive control up to about 250 Hz, as shown in Figure 9.

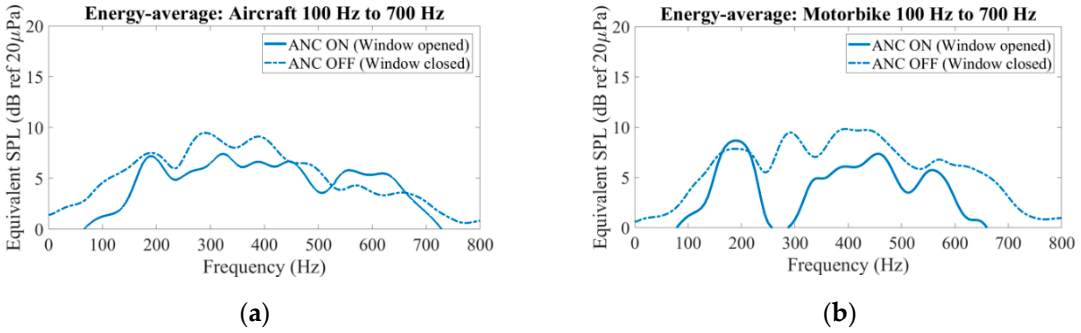

Figure 9. *Cont.*

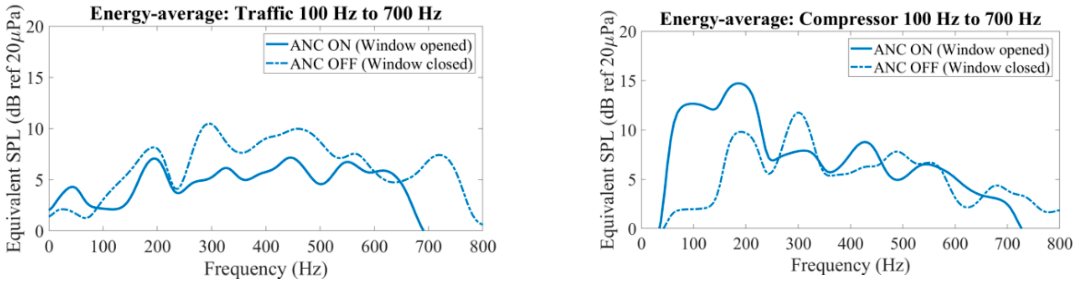

(**c**) (**d**)

Figure 9. Attenuation in dB as a function of frequency during ANC ON (window opened) and ANC OFF (window closed) for (**a**) aircraft, (**b**) motorbike, (**c**) traffic, and (**d**) compressor noise types.

4. Discussion and Conclusions

An active control method for controlling low-frequency urban noise while maintaining natural ventilation in a building was devised. Four loudspeakers were affixed to a frame surrounding a top-hung ventilation window in a full-sized mock-up apartment room. The active control system with a fully opened window achieved similar noise reduction to a fully closed window for aircraft noise, whereas active attenuation for traffic and motorbike noise was not too far off from passive insulation. In an extreme example, active attenuation of low-frequency compressor noise significantly outperformed that of a fully closed window. This highlights a potential scenario for low-frequency noise control through apertures beyond the domestic setting.

However, it is important to note that the upper frequency limit of the active control is dependent on the distance between the control loudspeakers [21,24] and appears to be related to the smallest dimension of the opening, as reported in [25]. In the top-hung window shown, the theoretical limit would be based on one wavelength of the shortest opening (~0.4 m), which is about 850 Hz. Besides the frequency limit, the directivity of the control loudspeaker becomes critical as the frequency increases, which would have implications on the placement of the loudspeakers and be worth further investigation. Moreover, only a single top-hung window was affixed with the active control system, potentially allowing low-frequency noise to leak into the interior through other, albeit closed, window panels. Expansion of the system to all available top-hung windows in the window system could be investigated next.

Despite the limitations, the attenuation results obtained from a single top-hung window are promising, especially for noise types with dominant low-frequency content, such as jet aircrafts and compressor noise. Although placement of control sources at the edge of the window frame was previously found to not be optimal [21], a tradeoff to obtain improved low-frequency performance and reduced visual obstruction could be worthwhile.

This ANC window system can also be a solution to the urban planner's dilemma of balancing the proximity and orientation of residential buildings to urban transport infrastructure. Optimizing the orientation of naturally ventilated buildings for wind flow, solar heat gain, and air temperature [26] would not be bogged down by the consideration of noise propagation. Moreover, the ANC window also provides an avenue for the indoor soundscaping of naturally ventilated buildings, whereby unwanted noise can be removed using selective algorithms [11,12] and wanted sounds can be introduced or amplified via the same loudspeakers that deliver the anti-noise. This element of controllability with an ANC system aligns well with the concept of adaptive acoustic comfort, suggested by Torresin et al. [9], which could be worth further investigation.

Author Contributions: Conceptualization, B.L. and W.-S.G.; methodology, B.L.; software, D.S.; investigation, B.L. and D.S.; validation, B.L., V.B., S.W. and D.S.; writing—original draft preparation, B.L.; writing—review and editing, D.S., V.B., S.W. and W.-S.G.; supervision, W.-S.G.; funding acquisition, W.-S.G.; project administration K.L. and I.L. All authors have read and agreed to the published version of the manuscript.

Funding: This research is supported by the Singapore Ministry of National Development and the National Research Foundation, Prime Minister's Office under the Cities of Tomorrow (CoT) Research Programme (CoT Award No. COT-V4-2019-1). Any opinions, findings, and conclusions or recommendations expressed in this material are those of the author(s) and do not reflect the views of the Singapore Ministry of National Development and National Research Foundation, Prime Minister's Office, Singapore.

Acknowledgments: The authors would like to thank Jerry Aw and Ng Kian Wee from the JTC Corporation for their assistance in the collection of the noise samples. We would also like to thank Masaharu Nishimura and Steve Elliott for their comments and suggestions.

Conflicts of Interest: The authors declare no conflict of interest. The funders had no role in the design of the study; in the collection, analyses, or interpretation of data; in the writing of the manuscript, or in the decision to publish the results.

References

1. World Health Organization Regional Office for Europe. *Environmental Noise Guidelines for the European Region*; The Regional Office for Europe of the World Health Organization: Copenhagen, Denmark, 2018; ISBN 9789289053563.
2. Murphy, E.; King, E.A. *Environmental Noise Pollution*; Elsevier: Amsterdam, The Netherlands, 2014; ISBN 9780124115958.
3. De Salis, M.H.F.; Oldham, D.J.; Sharples, S. Noise control strategies for naturally ventilated buildings. *Build. Environ.* **2002**, *37*, 471–484. [CrossRef]
4. Tang, S.-K. A Review on Natural Ventilation-enabling Façade Noise Control Devices for Congested High-Rise Cities. *Appl. Sci.* **2017**, *7*, 175. [CrossRef]
5. Torresin, S.; Albatici, R.; Aletta, F.; Babich, F.; Oberman, T.; Siboni, S.; Kang, J. Indoor soundscape assessment: A principal components model of acoustic perception in residential buildings. *Build. Environ.* **2020**, *182*, 107152. [CrossRef]
6. International Organization for Standardization. *ISO 12913-1: Acoustics—Soundscape—Part 1: Definition and Conceptual Framework*; International Organization for Standardization: Geneva, Switzerland, 2014.
7. International Organization for Standardization. *ISO/TS 12913-2: Acoustics—Soundscape—Part 2: Data Collection and Reporting Requirements*; International Organization for Standardization: Geneva, Switzerland, 2018.
8. International Organization for Standardization. *ISO/TS 12913-3: Acoustics Soundscape, Part. 3: Data Analysis*; International Organization for Standardization: Geneva, Switzerland, 2019.
9. Torresin, S.; Albatici, R.; Aletta, F.; Babich, F.; Oberman, T.; Kang, J. Acoustic Design Criteria in Naturally Ventilated Residential Buildings: New Research Perspectives by Applying the Indoor Soundscape Approach. *Appl. Sci.* **2019**, *9*, 5401. [CrossRef]
10. Ranjan, R.; He, J.; Murao, T.; Lam, B.; Gan, W.-S. Selective Active Noise Control System for Open Windows using Sound Classification. In Proceedings of the INTER-NOISE and NOISE-CON Congress and Conference Proceedings, InterNoise16, Hamburg, Germany, 21–24 August 2016; pp. 482–492.
11. Shi, D.; Gan, W.-S.; Lam, B.; Wen, S. Feedforward Selective Fixed-filter Active Noise Control: Algorithm and Implementation. *IEEE/ACM Trans. Audio Speech Lang. Process.* **2020**, *28*, 1479–1492. [CrossRef]
12. Wen, S.; Gan, W.-S.; Shi, D. Using empirical wavelet transform to speed up selective filtered active noise control system. *J. Acoust. Soc. Am.* **2020**, *147*, 3490–3501. [CrossRef] [PubMed]
13. Lam, B.; Shi, D.; Gan, W.-S.; Elliott, S.J.; Nishimura, M. Active control of broadband sound through the open aperture of a full-sized domestic window. *Sci. Rep.* **2020**, *10*, 10021. [CrossRef] [PubMed]
14. Samarasinghe, P.N.; Zhang, W.; Abhayapala, T.D. Recent Advances in Active Noise Control Inside Automobile Cabins: Toward quieter cars. *IEEE Signal. Process. Mag.* **2016**, *33*, 61–73. [CrossRef]
15. Cheer, J.; Elliott, S.J. Multichannel control systems for the attenuation of interior road noise in vehicles. *Mech. Syst. Signal. Process.* **2015**, *60–61*, 753–769. [CrossRef]
16. Elliot, S.J.; Nelson, P.A.; Stothers, I.M.; Boucher, C.C. In-flight experiments on the active control of propeller-induced cabin noise. *J. Sound Vib.* **1990**, *140*, 219–238. [CrossRef]
17. Chang, C.-Y.; Siswanto, A.; Ho, C.-Y.; Yeh, T.-K.; Chen, Y.-R.; Kuo, S.M. Listening in a Noisy Environment: Integration of active noise control in audio products. *IEEE Consum. Electron. Mag.* **2016**, *5*, 34–43. [CrossRef]

18. Murao, T.; Nishimura, M. Basic Study on Active Acoustic Shielding. *J. Environ. Eng.* **2012**, *7*, 76–91. [CrossRef]
19. Murao, T.; Nishimura, M.; Sakurama, K.; Nishida, S. Basic study on active acoustic shielding (Improving noise-reducing performance in low-frequency range). *Mech. Eng. J.* **2014**, *1*, EPS0065. [CrossRef]
20. Lam, B.; Shi, C.; Shi, D.; Gan, W.-S. Active control of sound through full-sized open windows. *Build. Environ.* **2018**, *141*, 16–27. [CrossRef]
21. Lam, B.; Elliott, S.; Cheer, J.; Gan, W.-S. Physical limits on the performance of active noise control through open windows. *Appl. Acoust.* **2018**, *137*, 9–17. [CrossRef]
22. EN ISO 16283-3. *Acoustics—Field Measurement of Sound Insulation in Buildings and of Building Elements Part 3 Façade Sound Insulation*, 1st ed.; International Organization for Standardization: Geneva, Switzerland, 2016.
23. Kuo, S.M.; Morgan, D.R. *Active Noise Control Systems: Algorithms and DSP Implementations*; Wiley: Hoboken, NJ, USA, 1996.
24. Elliott, S.J.; Cheer, J.; Lam, B.; Shi, C.; Gan, W. A wavenumber approach to analysing the active control of plane waves with arrays of secondary sources. *J. Sound Vib.* **2018**, *419*, 405–419. [CrossRef]
25. Wang, S.; Tao, J.; Qiu, X.; Pan, J. Mechanisms of active control of sound radiation from an opening with boundary installed secondary sources. *J. Acoust. Soc. Am.* **2018**, *143*, 3345–3351. [CrossRef] [PubMed]
26. Poh, H.J.; Koh, W.S.; Liu, E.; Zhao, W.; Tan, S.T. Modelling of Urban Heat Island and Noise Propagation in Singapore. In Proceedings of the 4th International Conference on Countermeasures to Urban Heat Island; Stephen Riady Centre, Singapore, 30 May–1 June 2016.